

## **Triosephosphate Isomerase by Consensus Design: Dramatic Differences in Physical Properties and Activity of Related Variants**

Brandon J. Sullivan<sup>\*</sup>, Venuka Durani<sup>†</sup> and Thomas J. Magliery<sup>†§</sup>

Departments of Chemistry<sup>†</sup> and Biochemistry<sup>‡</sup> and The Ohio State Biochemistry Program<sup>\*</sup>, The Ohio State University, 100 W. 18<sup>th</sup> Ave., Columbus, OH 43210, U.S.A.

<sup>§</sup>To whom correspondence should be addressed. Department of Chemistry, The Ohio State University, 100 W. 18<sup>th</sup> Ave., Columbus, OH 43210, U.S.A., Phone +1 (614) 247-8425, Fax +1 (614) 292-1685, E-mail magliery@chemistry.ohio-state.edu.

### **Supporting Information**

#### **Sequences**

##### **cTIM protein sequence – cleavable tag underlined**

MAHHHHHHGGENLYFQARTPFVGGNWKMNGTKAEAKELVEALKAKLPDDVEVVVAPPAVYL  
DTAREALKGSKIKVAAQNCYKEAKGAFTGEISPEMLKDLGADYVILGHSERRHYFGETDELVAK  
KVAHALEHGLKVIACIGETLEEREAGKTEEVVFRQTKALLAGLGDEWKNVVIAYEPVWAIGTGK  
TATPEQAQEVHAFIRKWLAENVSAEVAESVRILYGGSVKPANAKELAAQPDIDGFLVGGASLKP  
EFLDIINSRN\*

##### **ir-cTIM protein sequence – cleavable tag underlined.**

MGHHHHHHGHGGENLYFQARTPFVGGNFKLNGSKAEAKELVEALKAKLPDDVEVVVAPPATY  
LDYAREALKGSKIKVAAQNCYKKASGAFTGENSPEQIKDVGADYVILGHSERRHYFGETDEFVA  
KKVAHALEHGLKVIACIGETLEEREAGKTEEVVFRQTKALLAGLGDEWKNVVIAYEPVWAIGTG  
KTATPEQAQEVHAFIRKWLAENVSAEVAESVRILYGGSVKPANAKELAAQPDIDGFLVGGASLK  
PEFLDIINSRN\*

##### **ccTIM protein sequence – cleavable tag underlined**

MGHHHHHHGGENLYFQGSSGARTPLVAGNWKMNGTLAEAKELVEALAAKLPDDVEVVVAPPF  
TYLDQVRELLKGSKIAVGAQNCYKEDSGAFTGEISPAMLKDLGASYVILGHSERRQYFGETDEL  
VAKKVAAALAAGLTPILCVGETLEEREAGKTEEVVARQLKAVLAGLSDEWSNVVIAYEPVWAI

GTGKTATPEQAQEVHAFIRKWLAELSAEVAEKVRILYGGSVKPANAAELAAQPDIDGALVGGAS  
LKAEDFLAIINSRN\*

***S. cerevisiae* protein sequence – cleavable tag underlined**

MAHHHHHHGGENLYFQGSSGARTFFVGGNFKLNGSKQSIKEIVERLNTASIPENVEVVICPPATY  
LDYSVSLVKKPQVTVGAQNAYLKASGAFTGENSVVDQIKDVGAKWVILGHSERRSYFHEDDKFIA  
DKTKFALGQGVGVILCIGETLEEKKAGKTLDVVERQLNAVLEEVKDWTNVVVAYEPVWAIGTG  
LAATPEDAQDIHASIRKFLASKLGDKAASELRILYGGSSANGSNAVTFKDKADVDGFLVGGASLK  
PEFVDIINSRN

(Cleavage of the 6xHis-tag was only observed after cloning the linker, GSSG between the TEV recognition site and protein of interest.)

**Methods and Data**

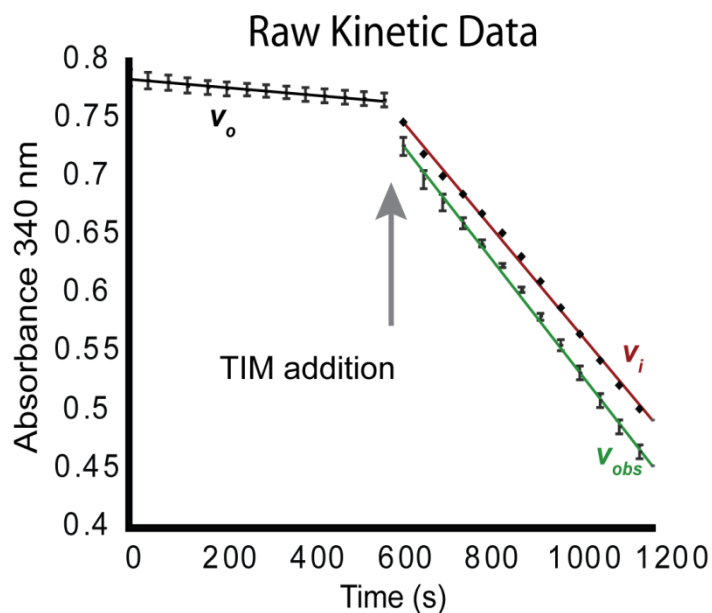
**Activity**

*Michaelis-Menten kinetics.* The  $k_{cat}$  and  $K_m$  were calculated using the assays described by Plaut and Knowles at 37 °C and pH 7.4. Our data were collected in 96-well plates using a Molecular Devices Spectramax M5 plate reader. The path length was calculated using known concentrations of NADH and Beer's Law with  $\epsilon = 6220 \text{ M}^{-1} \text{ cm}^{-1}$ . For a given volume, path lengths were consistent across the plate regardless of well position. The stock concentrations of DHAP and DL-GAP were determined enzymatically under conditions where each was the limiting reagent and the reaction was run to apparent completion. Here,  $A_f - A_i = \epsilon b(c_f - c_i)$ , where  $c_i$  is 0 and  $c_f$  is stoichiometrically related to the initial substrate concentration for the reaction. Reaction rates were determined by monitoring the appearance or disappearance of NADH at 340 nm when coupled to glyceraldehyde-3-phosphate dehydrogenase and  $\alpha$ -glycerol-3-phosphate dehydrogenase, respectively. Each reaction was monitored for ten minutes in the absence of TIM to calculate the background reaction rate ( $v_o$ ) from trace TIM contamination in the commercial coupling enzymes. After ten minutes, an aliquot of TIM was added to the well and the entire volume was pipetted 2 to 3 times to ensure proper mixing. The reaction rate ( $v_{obs}$ ) was then monitored for an additional 10 minutes. The initial reaction rate ( $v_i$ ) used to calculate the Michaelis-Menten parameters

was calculated as ( $v_i = v_{obs} - v_o$ ). Absorbance values were sampled every 45 seconds to limit photodegradation of the NADH. With GAP as the substrate, the reactions contained 0.1 M TEA buffer pH 7.4, 5 mM EDTA, 0.16 mM NADH, and 0 to 6.6 mM GAP. TIM concentration was 622 nM for cTIM, 1.24  $\mu$ M for ir-cTIM, 12.4 pM for ccTIM and 10 pM for yeast TIM. The concentration of  $\alpha$ -glycerol-3-phosphate dehydrogenase was optimized at 17  $\mu$ g mL<sup>-1</sup> to ensure it never limited  $v_{obs}$ . With DHAP as the substrate, the reactions contained 0.1 M TEA buffer pH 7.4, 5 mM EDTA, 6 mM sodium arsenate, 1 mM NAD<sup>+</sup>, 0 to 12 mM DHAP. TIM concentration was 1.24  $\mu$ M for cTIM, 1.24  $\mu$ M for ir-cTIM, 124 pM for ccTIM and 1.48 nM for yeast TIM. The concentration of glyceraldehyde-3-phosphate dehydrogenase was optimized at 0.2 mg mL<sup>-1</sup> to ensure it never limited  $v_{obs}$ . Triosephosphate isomerase concentrations were optimized such that  $v_{obs}$  would be linear for longer than 15 minutes, but statistically greater than  $v_o$ . Michaelis-Menten data sets were collected in triplicate and fitted in KaleidaGraph. The ccTIM  $K_m$  for DHAP was corrected for arsenate inhibition (see below). The Michaelis-Menten curves for the GAP reaction were performed in the presence and absence of 8.3 mM sodium arsenate. The  $K_i$  for arsenate was calculated to be 5 mM. This value was used to correct the  $K_m$  for DHAP from 5.3 to 2.4 mM for ccTIM.

#### *In vivo activity.*

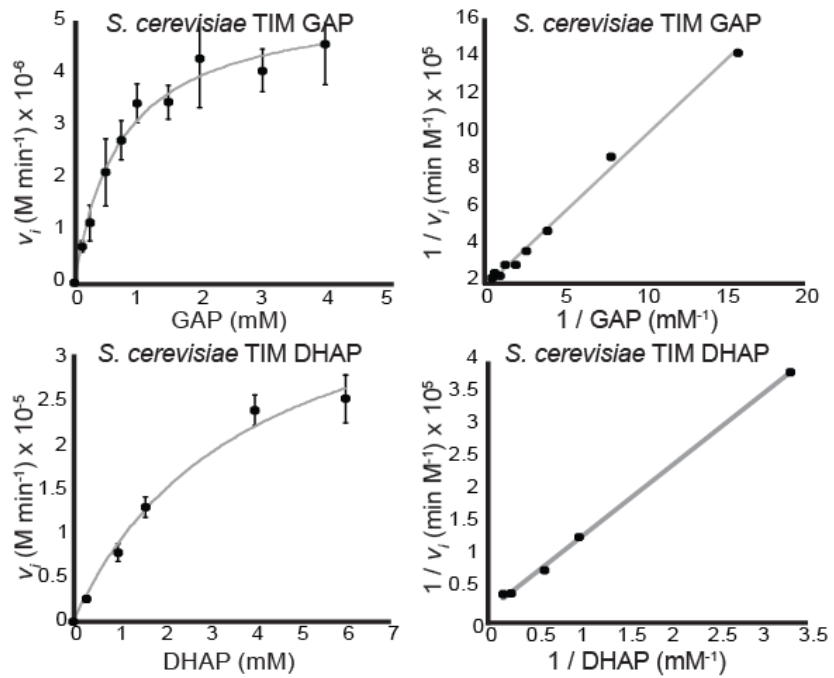
The Keio(DE3) strain was grown on minimal media agar plates lacking six carbon sugars. These plates were supplemented with M63 salts, 0.2 % w/v glycerol or lactate, 1 mg L<sup>-1</sup> thiamine, 80 mg L<sup>-1</sup> histidine and 50 mg L<sup>-1</sup> uracil. Plates contained ampicillin for plasmid selection and kanamycin for strain selection. Cells were grown for one to four days at 37 °C.



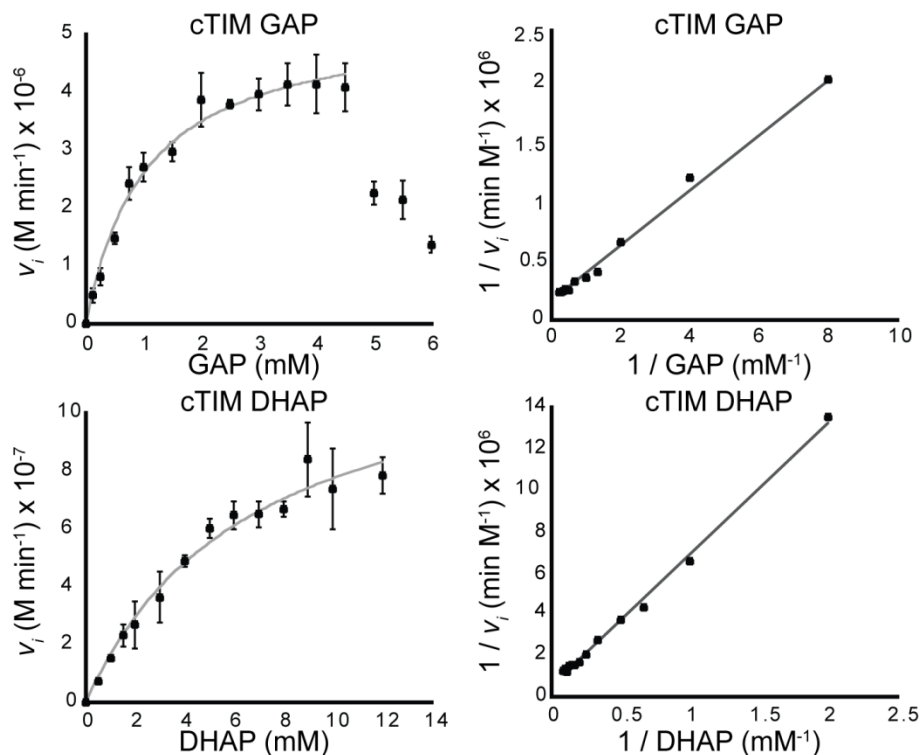
**Supplemental Figure 1.** Example kinetic data. The coupling enzymes, glyceraldehyde-3-phosphate dehydrogenase and  $\alpha$ -glycerol-3-phosphate dehydrogenase are both capable of interacting with TIM.<sup>a</sup> Crude commercial purifications result in preparations where both coupling enzymes are contaminated with highly active wild-type triosephosphate isomerase. Additionally, the enzymatically produced substrates are each contaminated with the isomerization product (i.e. GAP contains trace amount of DHAP and DHAP contains trace amounts of GAP). To account for these background reactions we collect data for 10 minutes before and after TIM addition as published by the JP Richard Lab.<sup>b</sup> The initial reaction rate ( $v_i$ ) used to calculate the Michaelis-Menten parameters was calculated as ( $v_i = v_{obs} - v_o$ ). Here we show triplicated data for a single GAP concentration. This process was performed for every data point.

<sup>a</sup>Srere (1987) Complexes of Sequential Metabolic Enzymes. *Ann. Rev. Biochem.* 56: 89-124.

<sup>b</sup>Go MK, Koudelka A, Amyes TL, & Richard JP (2010) Role of Lys-12 in catalysis by triosephosphate isomerase: a two-part substrate approach. *Biochemistry* 49:5377-5389.



**Supplemental Figure 2.** Michaelis-Menten and Lineweaver-Burke plots for wild-type *S.c.* TIM.



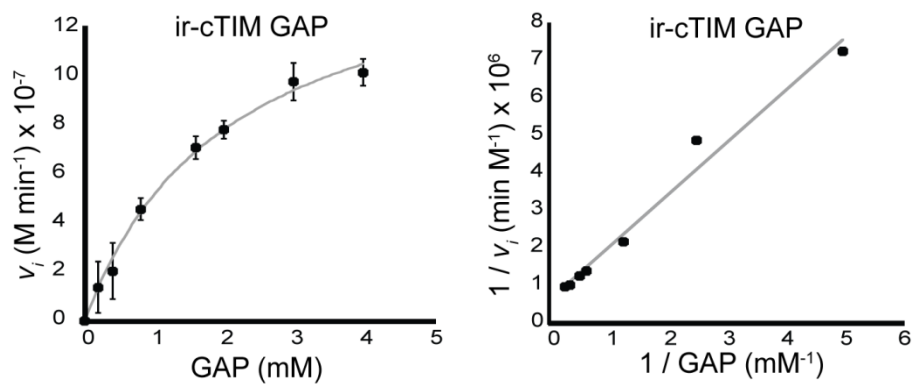
**Supplemental Figure 3.** Michaelis-Menten and Lineweaver-Burke plots for cTIM. For the forward (GAP) reaction, apparent  $v_{max}$  and  $K_m$  values were calculated from 0-4.5 mM GAP. The velocity of the reaction appeared to reach a maximum around 4.5 mM GAP and then decrease, suggesting substrate inhibition similar to that observed for rabbit TIM.<sup>c</sup> Fits performed with standard substrate inhibition models did not match the data well, suggesting the process of inhibition is more complex.<sup>d</sup>

$$rate = \frac{v_{max} [S]}{K_m + [S] + \frac{S^2}{K_i}}$$

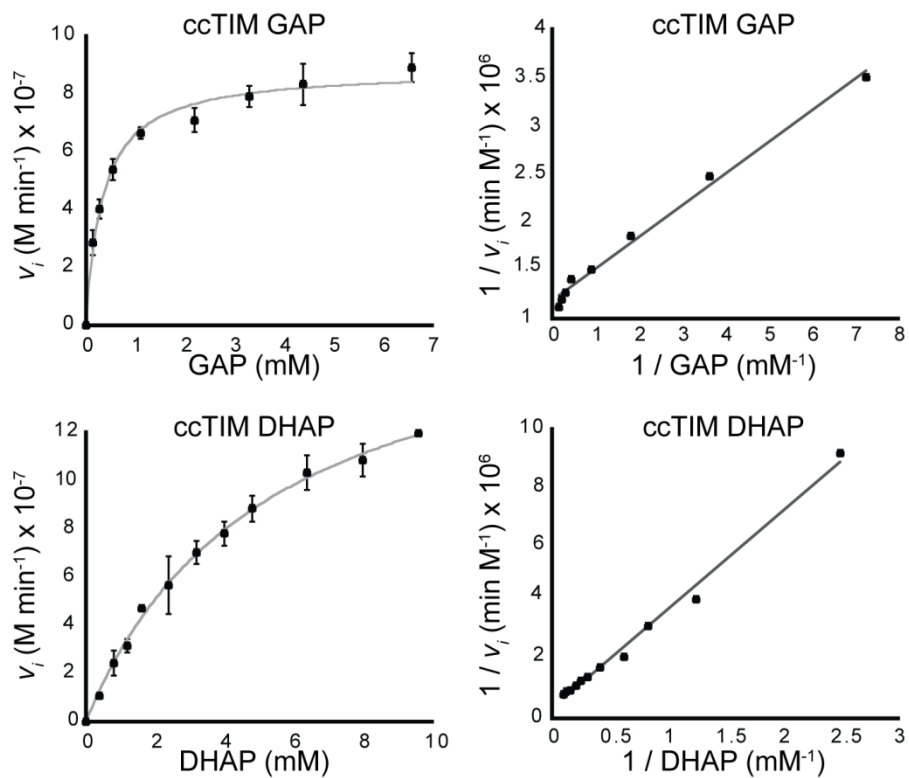
Because the reaction is coupled to reduction by NADH, it is much more likely that the inhibition is from substrate than from product. It has been suggested that this inhibition occurs when two substrate molecules bind the enzyme in a manner that inhibits activity. No evidence of substrate inhibition was seen in the other consensus-designed variants reported here.

<sup>c</sup>Chiang PK (1971) Allosteric properties of rabbit triosephosphate isomerase. *Life Sci* 10:831-9.

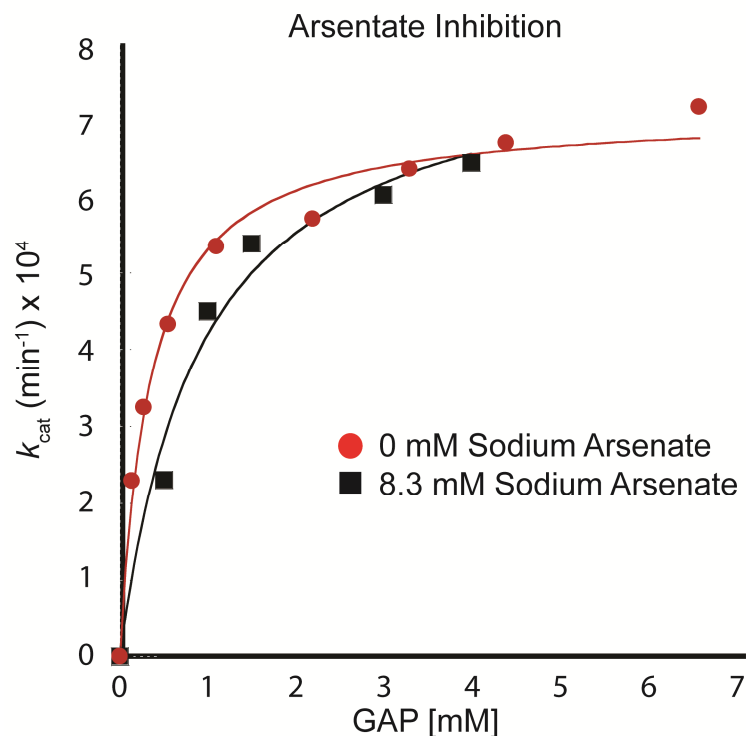
<sup>d</sup>Segel IR (Wiley 1993) *Enzyme Kinetics; behavior and analysis of rapid equilibrium and steady state enzyme systems.*



**Supplemental Figure 4.** Michaelis-Menten and Lineweaver-Burke plots for ir-cTIM. Values for ir-cTIM in the forward reaction were barely visible above the background reactions even at high enzyme concentrations. Using JP Richard's method of background subtraction we were able to calculate rates for the GAP reactions. When the same method was applied to the DHAP reaction,  $v_{obs} \approx v_o$ .



**Supplemental Figure 5.** Michaelis-Menten and Lineweaver-Burke plots for ccTIM.



**Supplemental Figure 6.** Arsenate inhibition of ccTIM. The Michaelis-Menten kinetics for ccTIM were measured in the absence and presence of 8.3 mM sodium arsenate. The increase in  $K_m$  with maintenance of  $v_{max}$  suggests arsenate is a competitive inhibitor, which is supported by previous data. The  $K_i$  for arsenate was estimated using the equation<sup>d</sup>:

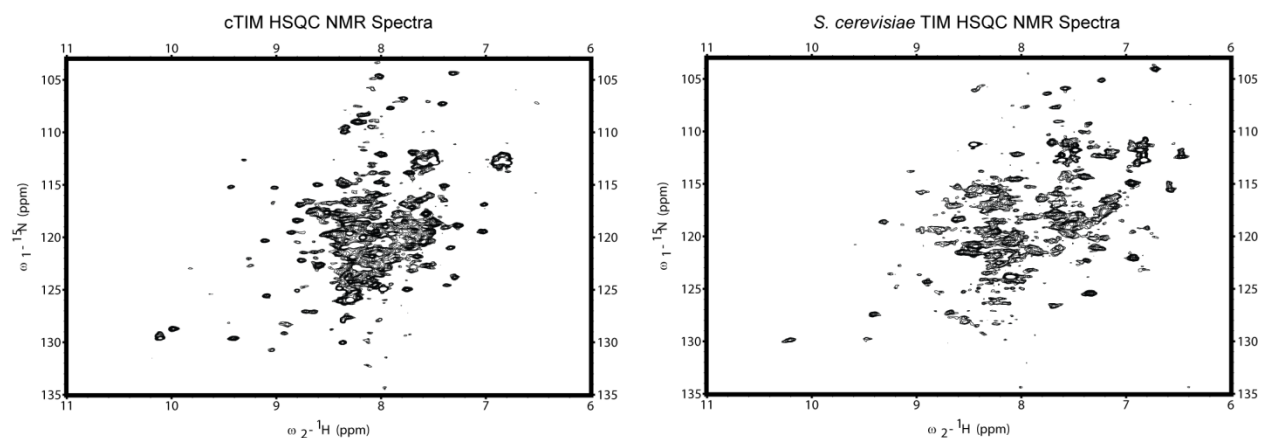
$$K_i = \frac{[I]}{\frac{K_{mAs}}{K_m} - 1}$$

The  $K_i$  was calculated as  $5 \pm 2$  mM. This value was used to adjust the  $K_m$  for DHAP using the equation<sup>d</sup>:

$$K_m = \frac{K_{mAs}}{\frac{[I]}{K_i} + 1}$$

This treatment yields an adjusted DHAP  $K_m$  of  $2.4 \pm 0.6$  mM.

<sup>d</sup>Segel IR (Wiley 1993) Enzyme Kinetics; behavior and analysis of rapid equilibrium and steady state enzyme systems.



**Supplemental Figure 7.**  $^1\text{H}$ ,  $^{15}\text{N}$ -HSQC NMR spectra of cTIM and yeast TIM. Seed cultures were grown in 2 $\times$ YT to saturation overnight. The next morning, cells were diluted 40-fold into 1 L minimal media supplemented with 5 mM sodium citrate, trace metals, 500  $\mu\text{M}$   $\text{MgSO}_4$ , 0.5% glucose, 0.1 mg thiamine and 1 g  $^{15}\text{NH}_4\text{Cl}$ . Cells were grown to  $\text{O.D.}_{600} \approx 0.75$  before induction with 0.1 mM IPTG. The proteins were purified as described in the Materials and Methods. Purified proteins were concentrated to 350  $\mu\text{M}$  in 50 mM sodium phosphate pH 7.4, 150 mM NaCl, 10 mM DTT and 1 mM TCEP. The  $^1\text{H}$ ,  $^{15}\text{N}$ -HSQC NMR spectra were obtained at 20  $^\circ\text{C}$  on a Bruker DRX 600 MHz.

**Supplemental Table 1.** Differences between cTIM and ccTIM.

| <i>S.c.</i> TIM <sup>a</sup><br>Site <sup>k</sup> | cTIM <sup>b</sup> | ccTIM <sup>c</sup> | R.E. <sup>d</sup> | Top 3 <sup>e</sup> | Top 3 % <sup>f</sup> | Henikoff <sup>g</sup> | Solvent Exp % <sup>h</sup> | Interface <sup>i</sup> | 2° structure <sup>j</sup> | Active     |
|---|-------------------|--------------------|-------------------|--------------------|----------------------|-----------------------|----------------------------|------------------------|---------------------------|------------|
| 6F  | F                 | L                  | 1.10              | LIF                | 81                   | 0                     | 0                          |                        | Sheet                     | 9.7 (E)    |
| 8G  | G                 | A                  | 1.42              | AGI                | 81                   | 0                     | 0                          |                        | Sheet                     | 7.1 (2PG)  |
| 17K   | K                 | L                  | 0.37              | LKR                | 48                   | -2                    | 40                         | X                      | Helix                     | 11.4 (K)   |
| 29T   | K                 | A                  | 0.39              | AKS                | 49                   | -1                    | 46                         |                        | Helix                     | 20.7 (K)   |
| 44A   | A                 | F                  | 1.14              | FAS                | 79                   | -2                    | 27 (0 dimer)               | X                      | Loop                      | 6.6 (K)    |
| 45T   | V                 | T                  | 0.96              | TVL                | 62                   | 0                     | 48 (0 dimer)               | X                      | Loop                      | 8.7 (K)    |
| 49Y   | T                 | Q                  | 0.24              | QAS                | 36                   | -1                    | 18                         | X                      | Helix                     | 12.9 (K)   |
| 50S   | A                 | V                  | 1.06              | VAL                | 74                   | 0                     | 0                          |                        | Helix                     | 10.4 (K)   |
| 53L   | A                 | L                  | 0.29              | LAK                | 50                   | -1                    | 7                          |                        | Helix                     | 15.8 (K)   |
| 60T   | K                 | A                  | 0.30              | AKG                | 44                   | -1                    | 14                         |                        | Sheet                     | 12.9 (K)   |
| 62G   | A                 | G                  | 1.62              | GAS                | 92                   | 0                     | 0                          |                        | Sheet                     | 9.6 (K)    |
| 70A   | A                 | D                  | 0.45              | DEA                | 49                   | -2                    | 11                         | X                      | Loop                      | 18.5 (H)   |
| 71S   | K                 | S                  | 0.44              | SKN                | 58                   | 0                     | 40                         | X                      | Loop                      | 20.3 (H)   |
| 81D   | E                 | A                  | 0.50              | AES                | 54                   | -1                    | 24                         | X                      | Helix                     | 17.8 (H)   |
| 89K   | D                 | S                  | 0.45              | SKT                | 44                   | 0                     | 34                         |                        | Sheet                     | 15.3 (K)   |
| 100S  | H                 | Q                  | 0.69              | QHA                | 47                   | 0                     | 33                         | X                      | Helix                     | 5.2 (H)    |
| 115F  | H                 | A                  | 0.95              | AHN                | 66                   | -2                    | 17                         |                        | Helix                     | 14.6 (H)   |
| 118G  | E                 | A                  | 0.68              | AEK                | 56                   | -1                    | 30                         |                        | Helix                     | 17.2 (H)   |
| 119Q  | H                 | A                  | 0.68              | AHN                | 55                   | -2                    | 20                         |                        | Helix                     | 18.2 (H)   |
| 122G  | K                 | T                  | 0.64              | TKI                | 59                   | -1                    | 4                          |                        | Sheet                     | 12.1 (H)   |
| 123V  | V                 | P                  | 1.76              | PVA                | 91                   | -2                    | 0                          |                        | Sheet                     | 9.3 (H)    |
| 125L  | A                 | L                  | 1.05              | LVA                | 76                   | -1                    | 0                          |                        | Sheet                     | 6.1 (H)    |
| 127I  | I                 | V                  | 1.68              | VIC                | 92                   | 1                     | 2                          |                        | Sheet                     | 2.8 (E)    |
| 144E  | G                 | A                  | 0.35              | AFG                | 41                   | 0                     | 24                         |                        | Helix                     | 11.0 (E)   |
| 147L  | T                 | L                  | 1.14              | LVI                | 79                   | -1                    | 0                          |                        | Helix                     | 9.8 (E)    |
| 150V  | L                 | V                  | 0.80              | VIA                | 61                   | 1                     | 2                          |                        | Helix                     | 10.5 (H)   |
| 155K  | G                 | S                  | 0.53              | SGL                | 53                   | 0                     | 62                         |                        | Loop                      | 18.9 (H)   |
| 158T  | N                 | S                  | 0.60              | SAK                | 61                   | 0                     | 42                         |                        | Loop                      | 14.5 (H)   |
| 195K  | N                 | Δ                  | NA                | NA                 | NA                   | NA                    | 36                         |                        | Loop                      | 18.9 (E)   |
| 196L  | V                 | L                  | 0.47              | LNK                | 53                   | 1                     | 17                         |                        | Helix                     | 16.2 (E)   |
| 203E  | S                 | K                  | 0.41              | KSA                | 45                   | 0                     | 40                         |                        | Helix                     | 16.5 (E)   |
| 218V  | K                 | A                  | 1.54              | AKER               | 60                   | -1                    | 27                         |                        | Helix                     | 13.3 (2PG) |
| 229F  | F                 | A                  | 1.26              | AFG                | 76                   | -2                    | 0                          |                        | Sheet                     | 6.2 (E)    |
| 238P  | P                 | A                  | 1.38              | APV                | 83                   | -1                    | 31                         |                        | Loop                      | 12.9 (2PG) |
| NA  | Δ                 | D                  | 0.88              | DSE                | 74                   | NA                    | NA                         |                        | Loop                      | NA         |
| 242D  | D                 | A                  | 0.57              | ADK                | 54                   | -2                    | 34                         |                        | Helix                     | 12.7 (2PG) |
| <i>Mutations Average</i>                          |                   |                    | 0.82              |                    |                      |                       | 20                         |                        |                           |            |
| <i>TIM Average</i>                                |                   |                    | 1.42              |                    |                      |                       | 17                         |                        |                           |            |

<sup>a</sup>The *S.c.* TIM residue and position that aligns with cTIM and ccTIM in the MSA; <sup>b</sup>The consensus TIM residue; <sup>c</sup>The curated consensus TIM residue; <sup>d</sup>The relative entropy for each position. Increasing relative entropies show increasing conservation within the amino acid distributions. <sup>e</sup>The three most common residues at each position; <sup>f</sup>The percent abundance of the three most common residues at each position; <sup>g</sup>The Henikoff score is a quantitative value to describe the conservativeness of a mutation based on phylogenetic analysis. Here, neutral mutations are given a score of 0, common mutations score positive while rare mutations are scored as negative values. <sup>h</sup>The solvent exposure of each residue was calculated in MOLMOL version 2K.2.0 with a 1.4 Å sphere. Buried residues generally have a solvent exposure of less than 10%; <sup>i</sup>X indicates residues that are within 5 Å of chain B in the crystal structure, 1YPI. Note that many of these residues are surface exposed, except positions 44 and 45 which pack into the second monomer; <sup>j</sup>The secondary structures based on DSS analysis in PyMOL; <sup>k</sup>The distances of all atoms from the mutated residues and the active site residues (K12, H95, E165), the 2PG inhibitor, and active site loop 6 (residues 166-176) were calculated in the inhibitor-bound crystal structure, 2YPI. The minimum distance is shown in Å with its closest active site neighbor (K-Lys12, H-His95, E-Glu165, 2PG-Inhibitor).